AIAA SciTech Forum
23-27 January 2023, National Harbor, MD & Online
AIAA SCITECH 2023 Forum
10.2514/6.2023-2254

Comparison of rotational and vibrational thermometry of detonation in microchannels

Sarang Bidwai*, Fynn Reinbacher† and James B. Michael ‡
Department of Mechanical Engineering, Iowa State University, Ames, Iowa, 50011

Chloe E. Dedic§
Department of Mechanical and Aerospace Engineering, University of Virginia, Charlottesville, Virginia, 22903

Vibrational and rotational temperatures in various detonation conditions involving diluted hydrogen-oxygen mixtures were studied in a microscale detonation tube using hybrid femtosecond/picosecond Coherent anti-Stokes Raman scattering (hybrid fs/ps CARS). Measured temperatures at various locations behind the shockwave were compared to Chapman-Jouguet conditions as predicted by equilibrium calculations. Simultaneous shadowgraphy was also employed to establish timing between the detonation wave and laser beams. Comparison between vibrational nitrogen and oxygen thermometry were made for detonations in the same gas mixture. Oxygen rotational temperature was measured and compared to vibrational temperature measured in a similar gas mixture.

I. Introduction

Pulsed detonation engines (PDEs) and rotating detonation engines (RDEs) have gained renewed interest in recent years. Detonation systems leverage the pressure rise for efficient conversion of the chemical energy stored in fuel/oxidizer mixture into usable energy [1]. Detonations generate pressure gain in the system, compared to pressure loss typically observed in deflagration combustion, which is a significant advantage. Therefore, utilizing the detonation phenomenon for propulsion and energy extraction has motivated many recent studies. There have been recent implementations of absorption spectroscopy in RDEs [2] and dual frequency comb spectroscopy for hypersonic combustion [3]. In a recent study, Hsu et al. have also successfully implemented OH planar laser-induced fluorescence (OH PLIF) imaging to rotating detonation combustor at megahertz-rate [4]. Coherent anti-Stokes Raman Scattering (CARS) has proven to be a strong candidate for investigating in-situ thermodynamic properties of detonation environments as it possesses high spatio-temporal accuracy [5]. Recent inquiries in the field have revealed a possibility of thermodynamic nonequilibrium in microscale detonations [6]. Numerous Monte-Carlo and direct numerical simulation studies have focused on evaluating the impact of such thermodynamic nonequilibrium and vibrational/rotational energy exchange on detonations [6–8]. Taylor et al. hypothesize that vibrational nonequilibrium caused by the presence of shockwaves can decrease chemical reaction rates, as vibrational relaxation timescales in stochiometric hydrogen-air detonations are comparable to ignition delay timescales [9, 10]. Shi et al. evaluated the effect of vibrational nonequilibrium on detonation cell size and found the vibrational relaxation times for chemical reactions play a significant role in predicting the detonation cell size [11]. Recent studies have also found unique phenomenon involving half reaction length sensitivity and vibrational nonequilibrium. According to Uy et al., half reaction lengths can be sensitive when considering vibrational nonequilibrium and increase in activation energy or decrease in time ratio of reactions [12, 13]. Accurate characterization of the energy distributions in the rotational and vibrational states of major species in detonation waves would help improve current models, thereby boosting our knowledge of these environments.

Coherent anti-Stokes Raman scattering (CARS) spectroscopy has been implemented to determine temperature and major species concentration in combustion environments with high accuracy and precision [14]. Early efforts utilized nanosecond laser sources to excite molecular transitions. However, scattering measurement and accuracy can be limited due to spectral broadening and interference from the nonresonant background, especially in high-pressure reacting flows [15]. In addition, picosecond and nanosecond CARS require knowledge of the collisional environment to determine the CARS signal generation accurately. Recent advancements in femtosecond solid-state lasers have resulted in the

*Graduate Student, AIAA Student Member
†Graduate Student, AIAA Student Member
‡Associate Professor, AIAA Member
§Assistant Professor, AIAA Member

development of ultrafast CARS, which can address some of the drawbacks of ns CARS. In particular, hybrid fs/ps CARS has been demonstrated to measure vibrational and rotational populations on a shot-to-shot basis [16–18]. It combines broadband excitation offered by femtosecond CARS and narrowband detection offered by picosecond CARS resulting in suppression of nonresonant background and minimizing effects of collisional energy transfer [19]. Hybrid fs/ps CARS has been applied to study vibrational-rotational nonequilibrium in environments such as a dielectric barrier discharge plasma [20] and microwave plasma-enhanced laminar flames [21].

The insight presented by Taylor et al, regarding the ignition delay time scales and vibrational relaxation timescales in hydrogen-air detonations were partiularly of interest as that would imply potential nonequilibrium in the detonation wave structure. Lower energy in vibrational modes of chemical species present will inhibit chemical reaction rates and cause incorrect prediction in chemical kinetics of these environments [10]. Furthermore, this could also hint toward the partial release of thermal energy beyond the sonic plane of a detonation which is not accessible to the detonation front. The goal of the current study is to measure and compare vibrational and rotational temperature in a microscale detonation as it exits a detonation tube to better understand the internal energy distributions of molecular species.

II. Methodology

A. Hybrid fs/ps CARS Theory

Hybrid fs/ps CARS signal is produced through a nonlinear, four-wave mixing process that requires three distinct laser pulses. Two of the pulses, namely pump (ω_1) and Stokes (ω_2), which are temporally short and spectrally broad, is used to excite the molecular rotational and/or vibrational transitions. A third pulse called probe (ω_3) which is frequency narrowed, is used to probe these transitions and generates the CARS signal. In this study, the pump and Stokes pulses are about 100 fs long, while the probe pulse is about 5.1 ps long. The third-order CARS polarization field is proportional to the Raman response of the molecule, which can be written as[5, 22]:

$$R(t) = c\sum_{i,f}\left(\frac{\partial\sigma}{\partial\Omega}\Delta\rho\right)_{i,f} e^{-(i\omega_{i,f}+\Gamma_{i,f})t}, \tag{1}$$

where $\frac{\partial\sigma}{\partial\Omega}$ is the Raman cross-section, $\Delta\rho$ the population difference between states in Raman transitions, $\omega_{i,f}$ the frequency of the state transition between states i and f, and $\Gamma_{i,f}$ the collisional linewidth. Raman transition cross-sections depend on Placzek-Teller coefficients as well as coefficients representing the overlap of upper and lower state energy wavefunctions. The simplified third-order polarization resulting from the molecular response can be written as [23]:

$$P^{3}(t,\tau_{2,3}) = \left(\frac{i}{\hbar}\right)^{3} E_3(t)\int_0^{\infty} dt_2\left[R(t_2)E_2^{*}(t+\tau_{2,3}-t_2)e^{(i(\omega_1-\omega_2))t_2}\right] \tag{2}$$

where E_i refers to the complex electric field envelope of the three corresponding laser pulses, $*$ denotes the complex conjugate, $\tau_{2,3}$ refers to the delay between probe and Stokes beams, and $R(t)$ is the time-dependent molecular Raman response.

To determine the temperature from CARS spectra, a simulation of rotational and vibrational CARS spectra for nitrogen and oxygen was implemented in Python. The computational code, named fspyCARS, consisted of subroutines for molecular energy levels, transition frequencies, Raman response, collisional linewidths (Modified Exponential Gap model), and optimization methods used for fitting experimental data. The algorithm implementation follows those implemented by Stauffer [24], Dedic [5, 23], and the original CARSFT code[25].

B. CARS Experimental Setup

The schematic of the hybrid fs/ps CARS experimental setup is shown in Figure 1a. A 1 kHz-rate regeneratively-amplified Ti:sapphire laser (Astrella F, Coherent) was used to produce the pump, Stokes, and probe beams from 7 W of total output. The pump and Stokes beams are used directly for rotational CARS and consist of 140 cm^{-1}, 100 fs pulses centered at 800 nm with single-shot energy of about 200 μJ. For vibrational thermometry, an optical parametric amplifier (TOPAS) was used to generate a 674 nm or 711 nm broadband beam which was used as the pump beam. The probe beam was generated using a Second Harmonic Bandwidth Compressor (SHBC), producing a frequency-narrowed 2.9 cm^{-1}, 5.1 ps pulse with single-shot energy of 100 μJ. This custom SHBC is the same used by Dedic and Michael [21], and the first use for hybrid fs/ps CARS probe beams was by Kearney and Scoglietti [20, 26]. The probe pulse was delayed using a motorized delay stage. The three beams were then focused using one lens consistent using a folded BOXCARS phase-matching configuration. An angle-tuned RazorEdge Filter (Semrock) was used to eliminate scattering from the 400 nm probe beam. The CARS signal was resolved using a 0.303 m spectrometer (Shamrock SR-303i, Andor) and collected using an EMCCD camera (Newton DU970, Andor). A 1:10 optical chopper system (MC2000B, Thorlabs) was used to ensure the acquisition of a single-shot signal and keep the sensor clean. This was necessary due to the large dynamic range between pulses prior to and properly timed with the transient detonation event.

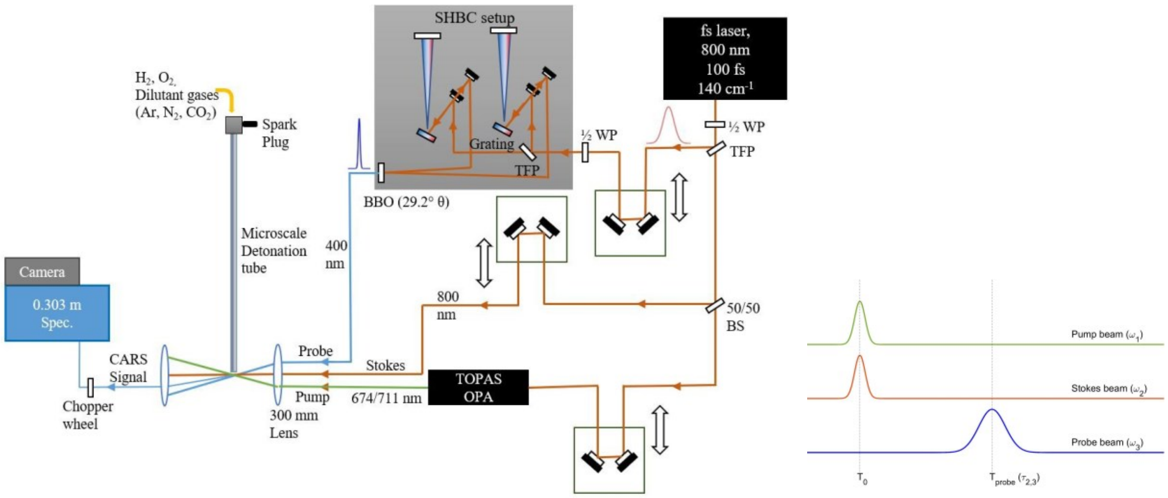

(a)

(b)

Fig. 1 (a) Schematic of Hybrid fs/ps CARS for vibrational CARS (VCARS) thermometry. Abbreviations: WP = waveplate, BBO = Beta Barium Borate crystal, OPA = optical parametric amplifier, TFP = thin film polarizer, BS = beam splitter. (b) Timing of pump, Stokes, probe beams.

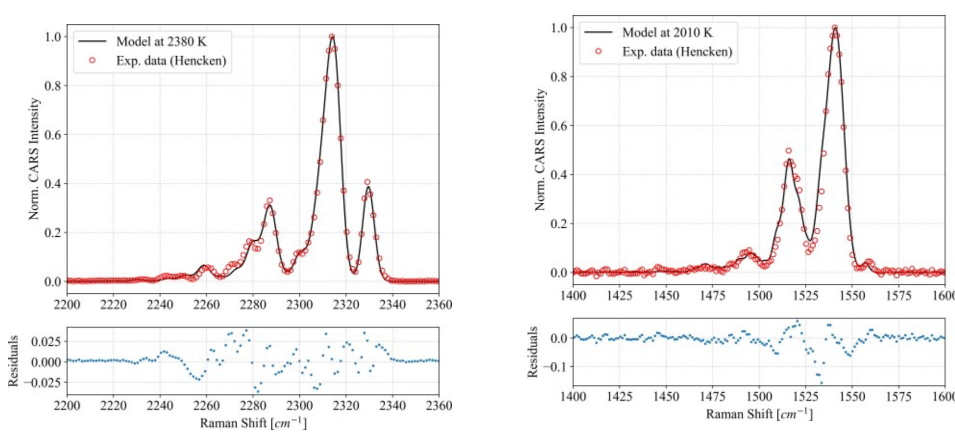

(a)

(b)

Fig. 2 (a) Temperature fit of N_2 vibrational CARS at 15 probe delay (b) Temperature fit of O_2 vibrational CARS at 15 ps probe delay

To verify the CARS setup and model, thermometry was conducted on relevant adiabatic hydrogen-air/hydrogen-oxygen-argon flame in a Hencken burner [22]. Pulse preparation parameters were confirmed from the adiabatic flame and non-resonant scans in argon. These included frequency chirp in the probe pulse, probe delay, and wavelength calibration of the spectrometer which determined from a multi-parameter optimization routine. The optimized parameters were used to generate a library of CARS spectra as a function of temperature. A fitting routine was implemented to determine best-fit temperatures by minimizing the ℓ^2-norm of residuals between CARS spectra and the library.

C. Microscale detonation tube setup

The detonation tube setup consisted of a 4.6 mm inner diameter, 0.6 m long stainless steel tube. Mass flow controllers (Alicat) were used to control the mass flow rates of gases which were premixed in a manifold. The mixture was transported through a meter-long stainless-steel tubing before the detonation tube. A premixed hydrogen-oxygen (and dilutant gas) mixture was ignited using a spark produced by a typical automobile spark plug setup, consisting of an ignition coil powered by a DC power supply. The timing of the spark and cameras was determined using BNC 577 pulse generator, which was synchronized with the laser system. To ensure no signal from cold gas outside the microchannel was produced, a shroud with Ar flow was positioned around the exit of the detonation tube. To monitor the detonation wave position at the tube exit, simultaneous shadowgraphs were acquired using the redirected probe beam after the signal was produced. This ensured the correct timing between the laser pulse and the detonation wave. The shadowgraphy setup was imaged using a monochrome CCD camera (Point Grey Chameleon).

III. Results and Discussion

A. Vibrational Thermometry

The experimental and best-fit spectra of N_2 and O_2 vibrational temperature for adiabatic Hencken flame are shown in Fig. 2. In detonation tube, a mixture of H_2-O_2-N_2 with equivalence ratio of 0.625 and nitrogen dilution of 33 % by vol., was investigated using both N_2 and O_2 vibrational CARS. Chapman-Jouguet (C-J) temperature of this mixture was found to be 3200 K from NASA Chemical Equilibrium with Applications (CEA) calculation. To verify the performance of the CARS thermometry for N_2 and O_2, high temperature flames were examined in Hencken burner.

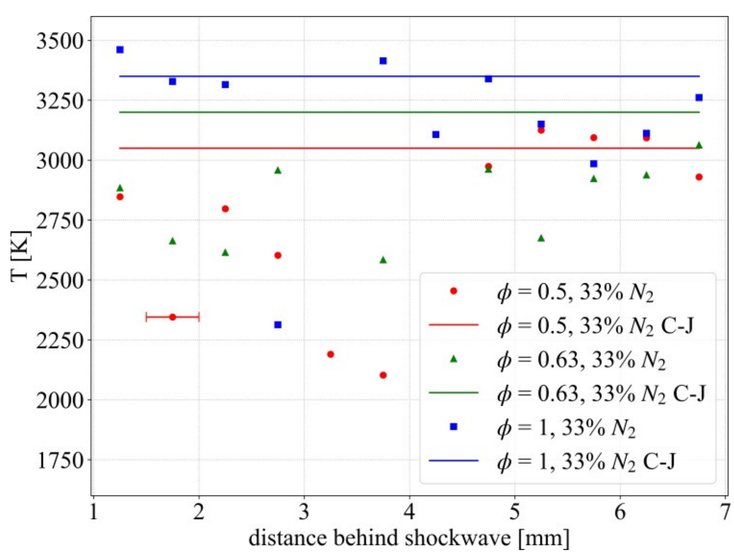

Fig. 3 N_2 vibrational CARS thermometry of gaseous detonations at several locations behind the shockwave as it expands out of a detonation tube.

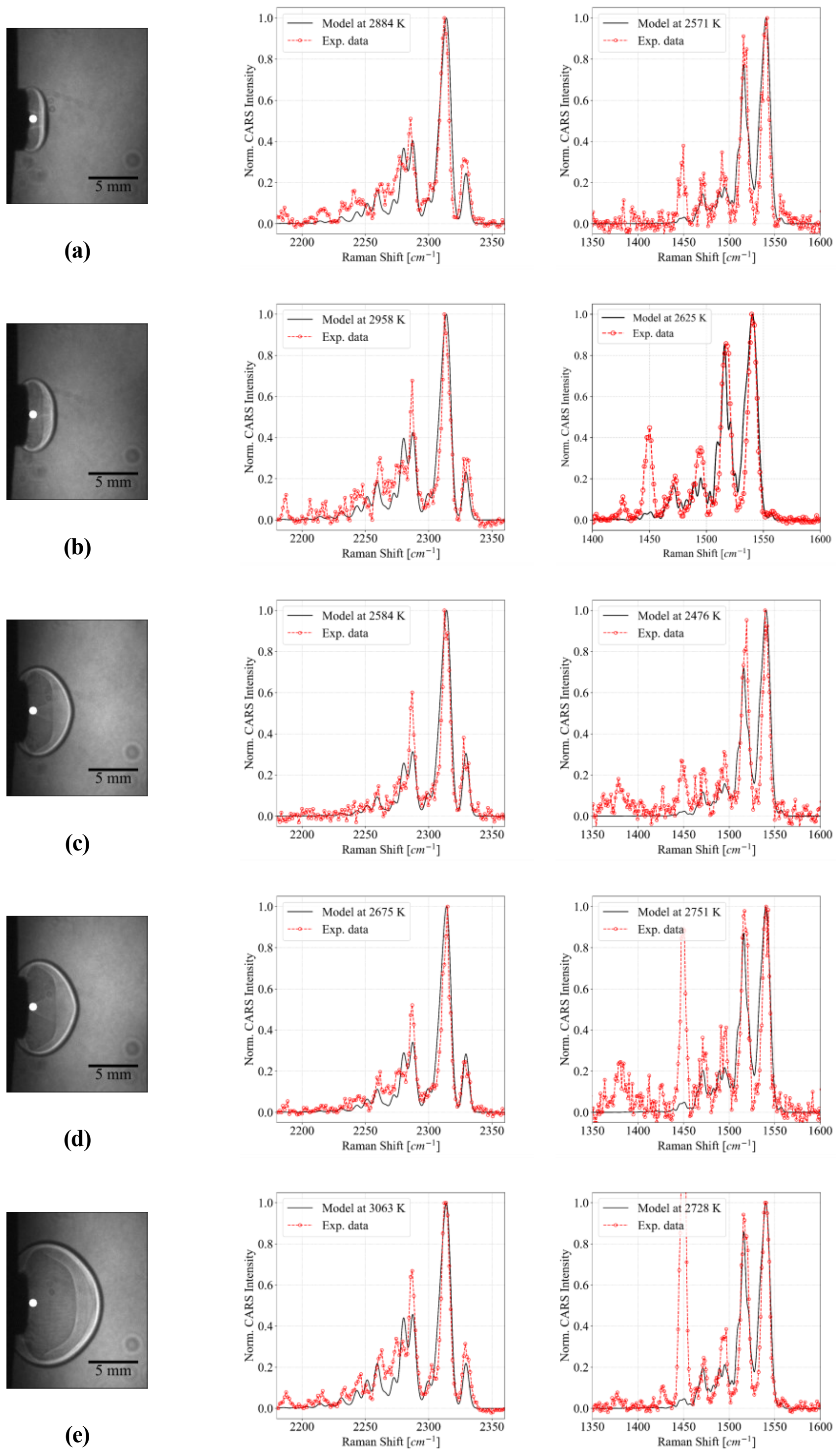

Fig. 4 Shadowgraphy, N_2, and O_2 CARS spectra at (a) 1.25 mm, (b) 1.75 mm, (c) 3.75 mm, (d) 5.25 mm, and (e) 6.75 mm behind the detonation front. The probe location was about 1 mm away from the exit(indicated by the white circle))

For these conditions, Fig. 5 shows the variation in the single-shot spectra of N_2 for location of 6.75 mm behind the shockwave. Averaging single-shot spectra by using the shadowgraphs to fix the wave position relative to the CARS measurement location increased signal-to-noise ratio (SNR) by nearly an order of magnitude at most locations.

Fig. 4 shows best-fit spectra of averaged signal at different locations in the detonation wave for both N_2 and O_2 Q-branch CARS. The signal acquired at a given location is averaged with all the shots with shockwave location within ± 0.25 mm of each other. Oxygen CARS spectra overlapped with the hydrogen rotational line at 1447 cm^{-1}, so this region was excluded in the fitting routine. Pressure for all of the detonation conditions was presumed to be equivalent to C-J pressure at all locations behind the shockwave. O_2 thermometry resulted in lower temperatures near the shockwave but comparable temperatures farther away, when compared to N_2 thermometry. The cause of lower O_2 temperature near the shockwave needs further investigation.

Two more gas mixtures were investigated using N_2 vibrational CARS to investigate the role of O_2 concentration on the temperature compared to their respective C-J temperatures. Fig 3 shows the measured temperature at different locations behind the shockwave for all three mixtures. Stoichiometric H_2-O_2 with 33 % N_2 resulted in temperatures close to C-J condition for the range of time delays and wave positions indicated.

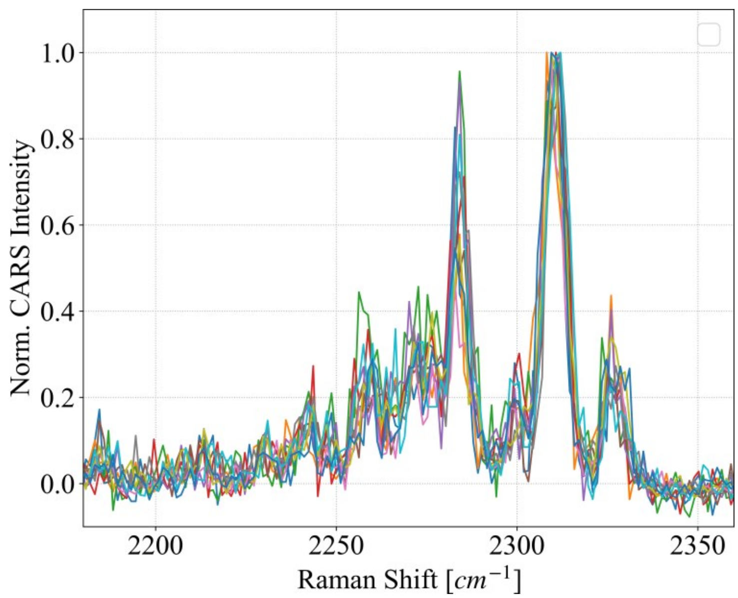

Fig. 5 Scatter of single-shot N_2 CARS signal at the location of 6.75 ± 0.25 mm

However, for lean cases significantly lower temperatures were observed. This result was unexpected as O_2 vibrational relaxation has significantly shorter time scales than N_2, which would imply temperatures comparable to C-J condition in excess O_2 environments. According to Taylor et al.[9], O_2 vibrational relaxation times of O_2 are much faster when compared to N_2. However Fig. 3 shows that for the stoichiometric condition, where O_2 concentration would be low, the measured temperatures correspond closely to C-J predictions, while lean cases are at a significantly lower temperature. One possible explanation for the lower temperature might be the location of deflagration to detonation transition (DDT) of the mixture. Lean mixtures have an extended DDT, which has been observed consistently in microchannels []. If the DDT occurs closer to the exit for lean conditions, rarefaction of the detonation wave might follow closely and lower the observed temperature at the probe volume.

B. Rotational Thermometry

Due to bandwidth limitations of the femtosecond laser, early probe delays were noted to be insensitive for O_2 rotational thermometry. To improve this, a probe delay of 30 ps was chosen based on the sensitivity to temperature as demonstrated in Fig. 6a. To avoid overlap between N_2 rotational and O_2 rotational transitions, N_2 was replaced withAr for rotational thermometry.

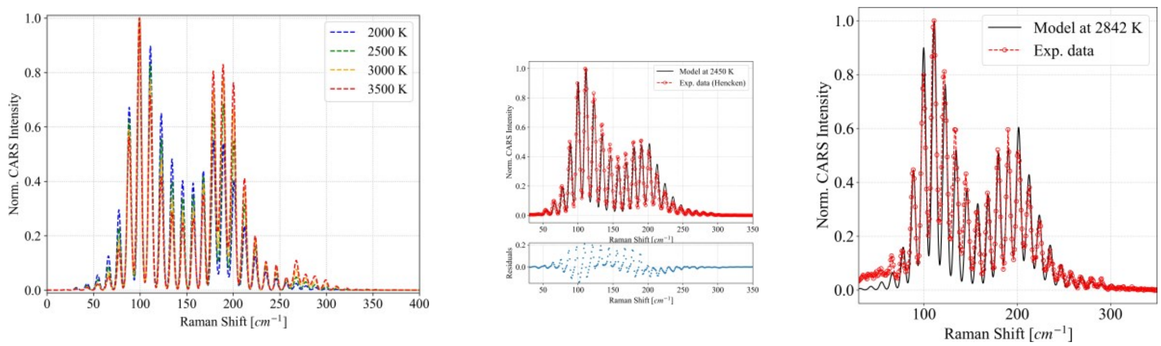

(a) (b) (c)

Fig. 6 (a) Sensitivity of O_2 rotational CARS at 30 ps **probe delay (b) Rotational temperature fit of O_2 CARS in an adiabatic Hencken flame with H_2-O_2-Ar mixture (c) Best-fit rotational temperature of H_2-O_2-Ar with C-J temperature of 3050 K 4.25 mm behind the shockwave**

Additionally, rotational CARS measurements proved challenging for timing close to shockwave transit. Significant probe beam scatter was observed, even with the sharp cut blocking filter, which made it difficult to measure the temperature reliably. Farther away from the shockwave temperature measurement are relatively consistent. Fig.6c shows best-fit temperature of a O_2 in a H_2-O_2-Ar mixture with equivalence ratio of 0.5 and Ar dilution of 55 % by volume, with a corresponding C-J temperature of 3050 K. The O_2 rotational temperature at this point is comparable to N_2 and O_2 vibrational temperature in mixtures with the same C-J temperature; however, rotational temperature closer to the shockwave still needs to be investigated. Since rotational temperature equilibrates much faster than vibrational temperature [27], if there is potential vibrational-rotational non-equilibrium in these detonation environments, it would be most pronounced near the shockwave. Therefore, investigating rotational temperature near the shockwave is crucial.

IV. Conclusion

Vibrational thermometry of N_2 and O_2 in various gaseous detonation conditons were conducted. Measured temperatures were compared to the theoretical Chapman-Jouguet temperatures for the mixtures. The evolution of temperature behind the shockwave as a detonation exits a microchannel was investigated. In oxygen-rich and dilute conditions vibrational temperatures significantly lower than C-J condition were observed. In stoichiometric and dilute conditions, vibrational temperature close to C-J condition was observed. Rotational temperature of O_2 was measured away from the shockwave and compared to relevant vibrational temperature measurements.

Further improvement in the rejection of probe scattering is necessary for rotational CARS measurements at short delays after the arrival of the detonation front. In addition, the role of products in hydrocarbon combustion on the post-detonation temperatures require more detailed understanding of both CO_2 and H_2O vibrational temperatures. Recent advances in quantitative CO_2 CARS offers the possibility of implementing simultaneous multi-species measurements. Thermometry in more complex gas mixtures involving relevant hydrocarbons such as ethylene will be investigated in the future.

Acknowledgments

This material is based upon work supported by the National Science Foundation under Grant No. 1839551. Additional instrumentation support was provided by ONR through award N000142012838. Any opinions, findings, and conclusions, or recommendations expressed in this material are those of the author(s) and do not necessarily reflect the views of the National Science Foundation or the Federal Government.

References

[1] Kailasanath, K., "Recent developments in the research on pulse detonation engines," *AIAA Journal*, Vol. 41, No. 2, 2003, pp. 145–159. https://doi.org/10.2514/2.1933.

[2] Rein, K. D., Roy, S., Sanders, S. T., Caswell, A. W., Schauer, F. R., and Gord, J. R., "Measurements of gas temperatures at 100 kHz within the annulus of a rotating detonation engine," *Applied Physics B: Lasers and Optics*, Vol. 123, No. 3, 2017, pp. 1–9. https://doi.org/10.1007/s00340-017-6647-5.

[3] Yun, D., Malarich, N. A., Cole, R. K., Egbert, S. C., France, J. J., Liu, J., Rice, K. M., Hagenmaier, M. A., Donbar, J. M., Hoghooghi, N., Coburn, S. C., and Rieker, G. B., "Hypersonic Combustion Diagnostics with Dual Comb Spectroscopy," 2022, pp. 1–8. URL http://arxiv.org/abs/2205.04891.

[4] Hsu, P. S., Slipchenko, M. N., Jiang, N., Fugger, C. A., Webb, A. M., Athmanathan, V., Meyer, T. R., and Roy, S., "Megahertz-rate OH planar laser-induced fluorescence imaging in a rotating detonation combustor," *Optics Letters*, Vol. 45, No. 20, 2020, p. 5776. https://doi.org/10.1364/ol.403199.

[5] Dedic, C. E., "Hybrid fs/ps coherent anti-Stokes Raman scattering for multiparameter measurements of combustion and nonequilibrium," Ph.D. thesis, 2017.

[6] Koo, H., Raman, V., and Varghese, P. L., "Direct numerical simulation of supersonic combustion with thermal nonequilibrium," *Proceedings of the Combustion Institute*, Vol. 35, No. 2, 2015, pp. 2145–2153. https://doi.org/10.1016/j.proci.2014.08.005, URL http://dx.doi.org/10.1016/j.proci.2014.08.005.

[7] O'Connor, P. D., Long, L. N., and Anderson, J. B., "The direct simulation of detonations," *Collection of Technical Papers - AIAA/ASME/SAE/ASEE 42nd Joint Propulsion Conference*, Vol. 2, 2006, pp. 911–921. https://doi.org/10.2514/6.2006-4411.

[8] Anderson, J. B., and Long, L. N., "Direct Monte Carlo simulation of chemical reaction systems: Prediction of ultrafast detonations," *Journal of Chemical Physics*, Vol. 118, No. 7, 2003, pp. 3102–3110. https://doi.org/10.1063/1.1537242.

[9] Taylor, B. D., Kessler, D. A., Gamezo, V. N., and Oran, E. S., "Numerical simulations of hydrogen detonations with detailed chemical kinetics," *Proceedings of the Combustion Institute*, Vol. 34, No. 2, 2013, pp. 2009–2016. https://doi.org/10.1016/j.proci.2012.05.045, URL http://dx.doi.org/10.1016/j.proci.2012.05.045.

[10] Taylor, B. D., Kessler, D. a., and Oran, E. S., "Estimates of Vibrational Nonequilibrium Time Scales in Hydrogen-Air Detonation Waves," 2013, pp. 1–6.

[11] Shi, L., Shen, H., Zhang, P., Zhang, D., and Wen, C., "Assessment of Vibrational Non-Equilibrium Effect on Detonation Cell Size," *Combustion Science and Technology*, Vol. 189, No. 5, 2017, pp. 841–853. https://doi.org/10.1080/00102202.2016.1260561, URL http://dx.doi.org/10.1080/00102202.2016.1260561.

[12] Uy, K. C., Shi, L., and Wen, C., "Chemical reaction mechanism related vibrational nonequilibrium effect on the Zel'dovichvon NeumannDÖring (ZND) detonation model," *Combustion and Flame*, Vol. 196, 2018, pp. 174–181. https://doi.org/10.1016/j.combustflame.2018.06.015, URL https://doi.org/10.1016/j.combustflame.2018.06.015.

[13] Uy, K. C. K., Shi, L., Hao, J., and Wen, C. Y., "Linear stability analysis of one-dimensional detonation coupled with vibrational relaxation," *Physics of Fluids*, Vol. 32, No. 12, 2020. https://doi.org/10.1063/5.0029468, URL https://doi.org/10.1063/5.0029468.

[14] Roy, G. D., Frolov, S. M., Borisov, A. A., and Netzer, D. W., "Pulse detonation propulsion: Challenges, current status, and future perspective," *Progress in Energy and Combustion Science*, Vol. 30, No. 6, 2004, pp. 545–672. https://doi.org/10.1016/j.pecs.2004.05.001.

[15] Seeger, T., Beyrau, F., Bräuer, A., and Leipertz, A., "High-pressure pure rotational CARS: Comparison of temperature measurements with O2, N2 and synthetic air," *Journal of Raman Spectroscopy*, Vol. 34, No. 12, 2003, pp. 932–939. https://doi.org/10.1002/jrs.1094.

[16] Prince, B. D., Chakraborty, A., Prince, B. M., and Stauffer, H. U., "Development of simultaneous frequency-and time-resolved coherent anti-Stokes Raman scattering for ultrafast detection of molecular Raman spectra," *The Journal of chemical physics*, Vol. 125, No. 4, 2006, p. 044502.

[17] Miller, J. D., Slipchenko, M. N., Meyer, T. R., Stauffer, H. U., and Gord, J. R., "Hybrid femtosecond / picosecond coherent anti-Stokes Raman scattering for high-speed gas-phase thermometry," *Optics Letters*, Vol. 35, No. 14, 2010, pp. 2430–2432.

[18] Dedic, C. E., Miller, J. D., and Meyer, T. R., "Dual-pump vibrational/rotational femtosecond/picosecond coherent anti-Stokes Raman scattering temperature and species measurements," *Optics Letters*, Vol. 39, No. 23, 2014, p. 6608. https://doi.org/10.1364/ol.39.006608.

[19] Dedic, C. E., Michael, J. B., and Meyer, T. R., "Hybrid fs/ps coherent anti-Stokes Raman scattering in a non-equilibrium environment initiated by a ns laser spark," *46th AIAA Plasmadynamics and Lasers Conference*, , No. June, 2015, pp. 1–10. https://doi.org/10.2514/6.2015-2962.

[20] Dedic, C. E., Meyer, T. R., and Michael, J. B., "Single-shot ultrafast coherent anti-Stokes Raman scattering of vibrational/rotational nonequilibrium," *Optica*, Vol. 4, No. 5, 2017, p. 563. https://doi.org/10.1364/optica.4.000563.

[21] Dedic, C. E., and Michael, J. B., "Thermalization dynamics in a pulsed microwave plasma-enhanced laminar flame," *Combustion and Flame*, Vol. 227, 2021, pp. 322–334. https://doi.org/10.1016/j.combustflame.2021.01.006, URL https://doi.org/10.1016/j.combustflame.2021.01.006.

[22] Hancock, R. D., Bertagnolli, K. E., and Lucht, R. P., "Nitrogen and hydrogen CARS temperature measurements in a hydrogen/air flame using a near-adiabatic flat-flame burner," *Combustion and Flame*, Vol. 109, No. 3, 1997, pp. 323–331. https://doi.org/10.1016/S0010-2180(96)00191-5.

[23] Miller, J. D., Roy, S., Slipchenko, M. N., Gord, J. R., and Meyer, T. R., "rotational hybrid femtosecond / picosecond coherent anti-Stokes Raman scattering," *Optics express*, Vol. 19, No. 16, 2011, pp. 15627–15640.

[24] Stauffer, H. U., Miller, J. D., Slipchenko, M. N., Meyer, T. R., Prince, B. D., Roy, S., and Gord, J. R., "Time- and frequency-dependent model of time-resolved coherent anti-Stokes Raman scattering (CARS) with a picosecond-duration probe pulse," *Journal of Chemical Physics*, Vol. 140, No. 2, 2014. https://doi.org/10.1063/1.4860475.

[25] Palmer, R. E., "The CARSFT computer code calculating coherent anti-Stokes Raman spectra: User and programmer information," Tech. rep., Sandia National Laboratories (SNL), Albuquerque, NM, and Livermore, CA (United States), feb 1989. https://doi.org/10.2172/6399189, URL http://www.osti.gov/servlets/purl/6399189/.

[26] Kearney, S. P., and Scoglietti, D. J., "Hybrid femtosecond/picosecond rotational coherent anti-Stokes Raman scattering at flame temperatures using a second-harmonic bandwidth-compressed probe," *Optics Letters*, Vol. 38, No. 6, 2013, p. 833. https://doi.org/10.1364/ol.38.000833.

[27] Eckbreth, A. C., *Laser diagnostics for combustion temperature and species*, CRC Press, 1996.